THE JOURNAL OF BIOLOGICAL CHEMISTRY VOL. 281, NO. 27, pp. 18463–18472, July 7, 2006

Essential Role of the B23/NPM Core Domain in Regulating ARF Binding and B23 Stability*

Received for publication, March 24, 2006, and in revised form, May 3, 2006 Published, JBC Papers in Press, May 5, 2006, DOI 10.1074/jbc.M602788200

Takeharu Enomoto[‡1,2], **Mikael S. Lindström**[‡1,3], **Aiwen Jin**[‡], **Hengming Ke**[§], **and Yanping Zhang**[‡¶‖4]

From the [‡]*Department of Radiation Oncology, the* [¶]*Lineberger Comprehensive Cancer Center, the* [‖]*Department of Pharmacology, and the* [§]*Department of Biochemistry and Biophysics, School of Medicine, University of North Carolina at Chapel Hill, Chapel Hill, North Carolina 27599-7512*

How cells coordinate inhibition of growth and division during genotoxic events is fundamental to our understanding of the origin of cancer. Despite increasing interest and extensive study, the mechanisms that link regulation of DNA synthesis and ribosomal biogenesis remain elusive. Recently, the tumor suppressor p14^{ARF} (ARF) has been shown to interact functionally with the nucleolar protein B23/NPM (B23) and inhibit rRNA biogenesis. However, the molecular basis of the ARF-B23 interaction is hitherto unclear. Here we show that a highly conserved motif in the B23 oligomerization domain is essential for mediating ARF binding *in vivo*. Mutagenesis of conserved B23 core residues (L102A, G105A, G107A) prevented B23 from interacting with ARF. Modeling of the B23 core indicated that substitutions in the GSGP loop motif could trigger conformational changes in B23 thereby obstructing ARF binding. Interestingly, the GSGP loop mutants were unstable, defective for oligomerization, and delocalized from the nucleolus to the nucleoplasm. B23 core mutants displayed increased ubiquitination and proteasomal degradation. We conclude that the functional integrity of the B23 core motif is required for stability, efficient nucleolar localization as well as ARF binding.

The tumor suppressor ARF is often mutated in human cancer at an overall frequency of ~40%, second only to that of p53 mutations (1). This extraordinarily high incidence of mutation of *ARF* is believed to be the result of the unusual organization of the gene in the genome. The human *ARF* gene resides at the chromosome 9p21 locus and, using an alternative reading frame, shares a common exon 2 with the CDK inhibitor p16^{INK4a} (2–5). The majority of mutations at the *ARF-INK4a* locus in human tumors involve homozygous deletions of the entire locus, causing simultaneous disruption of both genes and impairment of the two major tumor suppression pathways in mammalian cells, represented by the retinoblastoma protein Rb and the tumor suppressor protein p53, both of which are frequently inactivated in most, if not all, human cancers (6–9). ARF expression is elevated by stimulation from oncogenes such as Myc, E2F1, oncogenic Ras, adenovirus E1A, and v-Abl (10–14). Such observations led to a proposal that ARF mediates a p53-dependent checkpoint that, in response to hyperproliferative oncogenic signals, induces cell cycle arrest (15). Mechanistically, ARF binds MDM2 (16, 17), inhibits MDM2-mediated p53 ubiquitination and degradation (18), and activates p53. This is attained, at least in part, by blocking the nuclear export of both p53 and MDM2 (19, 20). Additional findings indicate that ARF has MDM2- and p53-independent functions in inducing both cell cycle arrest and apoptosis (21). Recently, two studies linked a function of ARF to ribosomal biogenesis and shed some light on the role of ARF in the nucleolus. The first study identified ARF as a factor involved in inhibiting the processing of rRNA (22) and this effect of ARF was independent of the function of MDM2 and p53. The second study identified that ARF physically interacts with, and functionally inhibits, the nucleolar protein B23/NPM (a.k.a. nucleophosmin, numatrin, NO38) by promoting B23 polyubiquitination and proteosomal degradation (23). Taken together, these two studies establish a previously unidentified nucleolar function for ARF in inhibiting ribosomal biogenesis.

B23 is an abundant nucleolar protein implicated in multiple cellular functions, including ribosome assembly and transport (24), centrosome duplication (25), molecular chaperone activity in preventing protein aggregation (26), and regulating the activity of p53 (27). B23 possesses endoribonuclease activity (28, 29) and cleaves the second internal transcribed spacer (ITS2) in 32 S pre-rRNA, generating mature 28 S rRNA (30). A previous study has suggested that B23 has a tumor suppression function through p53 (27). This conclusion was based on the observation that overexpression of B23 induces a p53-dependent cell cycle arrest in normal fibroblast cells. Other studies, however, have linked high level expression of B23 with uncontrolled cell growth, suggesting that B23 may have oncogenic potential (31–33). Overexpression of B23 in NIH-3T3 cells resulted in malignant transformation and caused tumorigenesis in nude mice (34). Such tumor cells also became resistant to UV-induced cell cycle arrest and apoptosis (35, 36). Conversely, mice lacking B23 die in early embryonic stages (37, 38), indicating an essential role for B23 in embryonic development. B23 belongs to the nucleoplasmin (Np)[5] superfamily of chaperones, which also includes proteins NO29, Npm3, ANO39, Mp62, and Np, the archetypal member of the family (39–41). Proteins belonging to the Np family have a conserved N-terminal core domain (Np-core). Although the exact role of the core is unclear, recent crystal structure studies have suggested that it mediates pentamer formation and histone binding (40, 42, 43). The ARF-B23 interaction has been confirmed recently, though the mechanistic explanation varies, by several other groups (44–46). These studies identify a genuine functional interaction between ARF and B23 and suggest a potential ARF-B23-rRNA pathway that, independent of the ARF-MDM2-p53 pathway, controls ribosomal biogenesis, and modulates growth arrest upon oncogenic insult. To gain further insights into the functions of ARF-B23 interaction, we investigated the ARF-B23 binding in detail and this report identifies amino acid sequences down to single residues in B23 required for ARF binding. More importantly,

* This study was supported by grants from the National Institutes of Health and the Leukemia Research Foundation. The costs of publication of this article were defrayed in part by the payment of page charges. This article must therefore be hereby marked "*advertisement*" in accordance with 18 U.S.C. Section 1734 solely to indicate this fact.

[1] Both authors contributed equally to this work.

[2] Supported in part by the Dept. of Surgery, St. Marianna University School of Medicine.
[3] Supported by a postdoctoral fellowship from the Swedish Research Council.

[4] Recipient of a Career Award in Biomedical Science from the Burroughs Wellcome Fund and a Howard Temin Award from the NCI, National Institutes of Health. To whom correspondence should be addressed. Tel.: 919-966-7713; Fax: 919-966-7681; E-mail: ypzhang@med.unc.edu.

[5] The abbreviations used are: Np, nucleoplasmin; GST, glutathione *S*-transferase; GFP, green fluorescent protein; wt, wild type; IVT, *in vitro* transcription/translation; NLS, nuclear localization signal; PBS, phosphate-buffered saline; HA, hemagglutinin.

the same ARF binding essential residues in B23 were also found to be required for B23 oligomerization, protein stability, and efficient nucleolar accumulation. A potential mechanism of how ARF inhibits B23 function will be discussed.

MATERIALS AND METHODS

Plasmids—pcDNA3-myc3-B23, B23-(117–294), B23-(196–294), and B23-(1–192) constructs were previously described (23). Novel B23 deletion mutants and point mutations were constructed by conventional PCR or PCR-mediated mutagenesis using pcDNA3-myc3-B23 as a template. B23 wild type, deletion, or point mutants were cloned in frame with GST in the pGEX-2T vector or inserted in-frame with GFP in the EGFP-N1 vector. PCR primer sequences and details for PCR are available upon request. All mutants were confirmed by direct DNA sequencing. ARF constructs and adenovirus were described elsewhere (16, 19).

Antibodies—Mouse monoclonal antibodies against B23 (Zymed Laboratories), actin (MAB1501, Chemicon International), FLAG (M2, Sigma), GST (Amersham Biosciences), and rabbit polyclonal antibodies against Myc (used in Fig. 1, Abcam) were purchased commercially. The affinity-purified rabbit polyclonal ARF antibody was described previously (16). Rabbit polyclonal Myc antibody was a gift from Dr. Yue Xiong (UNC, Chapel Hill). Horseradish peroxidase-conjugated donkey anti-mouse and anti-rabbit antibodies and rhodamine-red-conjugated donkey anti-mouse and anti-rabbit secondary antibodies were purchased from Jackson ImmunoResearch Laboratories.

Cell Lines and Transfection—U2OS (p53 wt, human osteosarcoma) was obtained from ATCC. Cells were transfected using Effectene (Qiagen) according to the manufacturer's instructions. In some experiments, actinomycin D (Sigma) was dissolved in 100% ethanol as a 5 mM stock, with a final concentration of 5 nM used for treatments (47). MG132 (Calbiochem) was dissolved in 100% ethanol as a 10 mM stock and a final concentration of 10 μM was used for treatments.

Immunoprecipitation and Western Blotting—Cells were harvested 24 h after transfection and lysed in Nonidet P-40 lysis buffer (50 mM Tris-HCl, pH 7.5, 150 mM NaCl, 0.5% Nonidet P-40, 50 mM NaF, 1 mM $NaVO_3$, 1 mM dithiothreitol, 1× protease inhibitor cocktail, 1 mM phenylmethylsulfonyl fluoride), and the supernatants were transferred to a new tube. Antibodies were added to the lysates, mouse monoclonal anti-HA antibody 30 μl/each, rabbit polyclonal anti-Myc antibody 0.7–1.0 μg/each, and samples were incubated from 2 h at room temperature to overnight at 4 °C. The samples were then washed three times with cold lysis buffer. The samples were dissolved in Laemmli buffer and analyzed by SDS-PAGE. Membranes were blocked in blocking solution (1× PBS-0.1% Tween-20 with 5–10% dry milk) for 2 h before incubation with primary antibodies as follows: mouse monoclonal antibodies against B23 (0.05 μg/ml), actin (1:125,000), Myc (30 μl/ml), or rabbit polyclonal antibody against ARF (0.2 μg/ml) and Myc (0.07–0.2 μg/ml) for 2 h at room temperature to overnight at 4 °C. Membranes were washed three times for 10 min each in 1× PBS-0.1% Tween-20 with shaking. Secondary antibody was added (horseradish peroxidase-conjugated anti-mouse (1:10,000) or anti-rabbit (1:20,000) antibodies) to the membrane and incubated with slow shaking for 1 h at room temperature. The membrane was washed three times for 10 min each with 1× PBS, 0.1% Tween-20 and 1× for 5 min with 1× PBS. Signals were detected by ECL (Amersham Biosciences), West-Pico, or West-Dura (Pierce) reagents.

Immunofluorescence and Live Cell Imaging—Cultured cells were seeded onto 6-well plates and transfected with plasmid DNA (0.3 μg/well). Twenty-four hours after transfection, cells were washed two times with 1× PBS and fixed in 4% formalin solution (Sigma Diagnostics) for 10 min. Cells were then washed with 1× PBS and subsequently in cold 1× PBS containing 0.2% Triton X-100 for 5 min at 4 °C, followed by incubation with 1× PBS containing 0.5% bovine serum albumin for 30 min prior to incubation with primary antibodies overnight. Cells were then incubated with fluorochrome-conjugated secondary antibody for 30 min and were covered by anti-fluorescent mounting medium (DAKO) and examined with an Olympus IX81 microscope fitted with appropriate fluorescence filters. For visualization in living cells, U2OS cells were seeded in 6-well plates followed by transfection with plasmids encoding wild-type or mutant B23 fused with EGFP at the C terminus and live cells were analyzed and photographed using the microscope described above.

Pulse Chase Experiment for Protein Half-life Assay—U2OS cells were seeded onto a 60-mm plate and transfected with a total of 0.7 μg of plasmid DNA. Twenty-four hours after transfection, cells were labeled with [^{35}S]methionine for 2 h, washed with warm 1× PBS, and chased by culturing in Dulbecco's modified Eagle's medium/10% fetal bovine serum media for the times indicated in each figure.

In Vivo Ubiquitination Assay—U2OS cells were transfected with plasmids expressing wild-type or mutant B23 proteins with or without a plasmid expressing HA-poly-Ub. Twenty hours after transfection, cells were treated with 10 μM (final concentration) of MG132 proteasome inhibitor for another 10 h. After harvest, cell pellets were resuspended in 100 μl of 50 mM Tris-HCl, pH 7.5, 0.5 mM EDTA, 1% SDS, 1/1000 1 M dithiothreitol, and boiled for 10 min. To the clarified denatured lysates, 1 ml of 0.1% Nonidet P-40 lysis buffer was added followed by immunoprecipitation and Western blotting.

In Vitro Transcription, Translation, and GST Pull-down Assay—*In vitro* transcription/translation (IVT) assays were performed essentially as previously described (16). Briefly, the coupled *in vitro* transcription and translation reactions were performed using the TNT kit as per the manufacturer's instructions (Promega). For *in vitro* binding assays individually translated proteins were mixed together and incubated at 30 °C for 30 min to allow binding to occur. At the end of the incubation, 200 μl of Nonidet P-40 lysis buffer was added to each binding reaction followed by immunoprecipitation with appropriate antibodies. Expression, purification, and elution of GST fusion proteins with glutathione were done according to the manufacturer's instructions (Amersham Biosciences). For GST pull-down assay, GST fusion proteins bound to glutathione-Sepharose 4B beads (Amersham Biosciences) were incubated and rotated overnight at +4 °C with *in vitro* translated protein in binding buffer (0.1% Nonidet P-40, 150 mM NaCl, 1 mM phenylmethylsulfonyl fluoride). Following extensive washing in binding buffer the beads were boiled and resuspended in SDS loading buffer and resolved on SDS-PAGE gel, followed by gel staining with Coomassie Brilliant Blue, drying, and autoradiography. For non-reducing SDS-PAGE as indicated, protein samples were loaded without heating and dithiothreitol.

Cell Proliferation Assays and siRNA—Cells were seeded in 6-well plates, and proliferation was measured by total cell count and absorbance measurement at 595 nm on total protein (Bradford assay) or using acid-extracted crystal violet stain from fixed cells. Knocking down B23 in 6-well plates using siRNA oligos was previously described (23). Rescue of B23 expression was done 72 h after siRNA transfection by GFP, B23-GFP, or mutant constructs using FuGENE 6 transfection reagent.

Crystal Structure Modeling—The structural model of N-terminal B23 was built on the basis of the structure of *Xenopus* NO38 (entry code

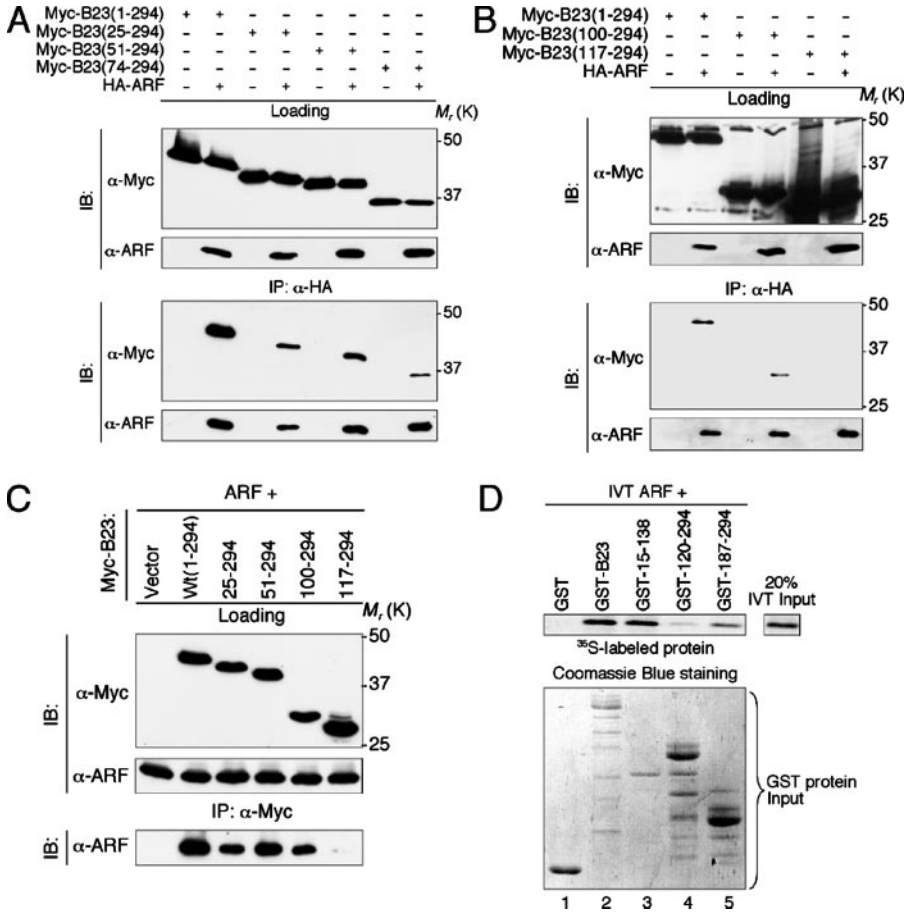

FIGURE 1. **ARF interacts with a short motif in the N-terminal oligomerization domain of B23.** *A* and *B*, N terminus of B23 is required for ARF binding. U2OS cells were either singly transfected with plasmids encoding wild-type Myc-B23 and Myc-tagged B23 N-terminal deletion mutants (25–294, 51–294, 74–294, 100–294) or cotransfected with various B23 constructs and HA-ARF, as indicated. Twenty-four hours after transfection, cell lysates were prepared and immunoprecipitated with anti-HA antibody 12CA5 (for ARF). The precipitates were resolved by SDS-PAGE, transferred to a nitrocellulose membrane, and blotted with an anti-Myc antibody 9E10 (for B23) and an anti-ARF antibody. Approximately 10% of cell lysate was shown as loading control. *IP*, immunoprecipitate; *IB*, immunoblot. *C*, interaction of ARF with B23 or B23 N-terminal deletion mutants were shown by reciprocal immunoprecipitation with anti-Myc antibody (for B23) and Western blotting with anti-ARF antibody. *D*, *in vitro* binding of ^{35}S-labeled ARF with GST-B23. ^{35}S-labeled ARF protein was produced with a coupled IVT system. Equal amounts of ^{35}S-labeled ARF protein were incubated with bacterial produced wild-type GST-B23 and various GST-B23 mutants as indicated. B23-bound ARF was detected by autoradiography, and the B23 input was shown by Coomassie Brilliant Blue staining. Lower fragments seen represent proteolytic degradation fragments emanating from the protease sensitive C-terminal region of B23, whereas no degradation is seen with the core fragment of B23-(15–138) known to be resistant to degradation.

1XB9, Protein Data Bank). The differences in the amino acid sequences were mutated by the program O (48), and the orientations of the side chains were manually adjusted in a Silicon Graphic system. The molecular model and interfacial interaction were presented by the program Ribbons (49).

RESULTS

ARF Interacts with a Short Motif in the N-terminal Oligomerization Domain of B23—We have previously shown that the N-terminal 113 amino acid residues of B23 interact with human p14ARF (ARF thereafter) (23). This area spans the entire B23 homo-oligomerization domain that has been mapped at residues 1–119 (50). To gain insight into the ARF-B23 interaction, we mapped the ARF binding site in B23 in detail using a series of B23 N-terminal deletion mutants. B23 with the first 24, 50, or 73 residues deleted retained the capacity to bind ARF, though the binding activity of the deletion mutants appeared to decrease with progressive deletion from the N terminus (Fig. 1*A*). The B23 mutant with the first 99 residues deleted (100–294) showed diminished ARF binding ability, indicating that it was either lacking part of the B23 sequence required for, or was otherwise interfering with, ARF binding (Fig. 1*B*). Consistent with previous reports (23, 45), deletion of the first 116 residues from B23 (117–294) eliminated ARF binding (Fig. 1, *B* and *C*). These results were identical to those obtained in an ARF-B23 *in vitro* binding assay (data not shown). Thus, it appears that a short sequence from residues 100–116 of B23 contains an element strictly required for ARF binding. It is notable that this short region has elsewhere been suggested to be a putative metal binding domain (51), and the region 90–117 was also found to be most important for the *in vitro* chaperone activity of B23 (50).

A previous study using bacterial produced GST-B23 suggested that a B23 fragment spanning residues 187–294 contains the ARF-binding site (46), which is at odds with this finding and with two previous studies showing that the ARF-B23 interaction requires B23 oligomerization domain (23) and the oligomerization and the acidic domains (45). To determine whether experimental conditions might be a factor in the differences, we carried out an assay using B23 produced in bacteria and ARF produced by coupled IVT and found that a B23 C-terminal fragment of 187–294 fused with GST was indeed able to interact with ARF *in vitro* (Fig. 1*D*, *lane 5*). Intriguingly, however, we found that a longer B23 fragment of 120–294 was unable to interact with ARF (Fig. 1*D*, *lane 4*), consistent with our *in vivo* co-immunoprecipitation data (Fig. 1, *B* and *C*). Thus, there may exist another ARF binding site in the B23 C terminus that is masked by the N-terminal sequences and that can be exposed under certain circumstances. In any case, we confirmed that the binding between ARF and the B23 N-terminal oligomerization domain is direct, as the B23 region 15–138 fused with GST is able to strongly interact with ARF *in vitro* (Fig. 1*D*, *lane 3*), and because that we could not detect B23 protein in the reticulocyte lysate used in this *in vitro* assay,[6] ruling out possible bridging by endogenous, full-length B23.

Identification of Residues in B23 Required for ARF Binding—B23 (NPM or NPM1) belongs to a specific class of acidic chaperone proteins that also includes NPM2 (52), NPM3 (53), and nucleoplasmin (39) collectively known as the nucleoplasmin family (Fig. 2*A*). The N-terminal region of B23 consists of an oligomerization domain followed by two highly acidic regions that are separated by a bipartite

[6] M. Lindstrom and Y. Zhang, unpublished observations.

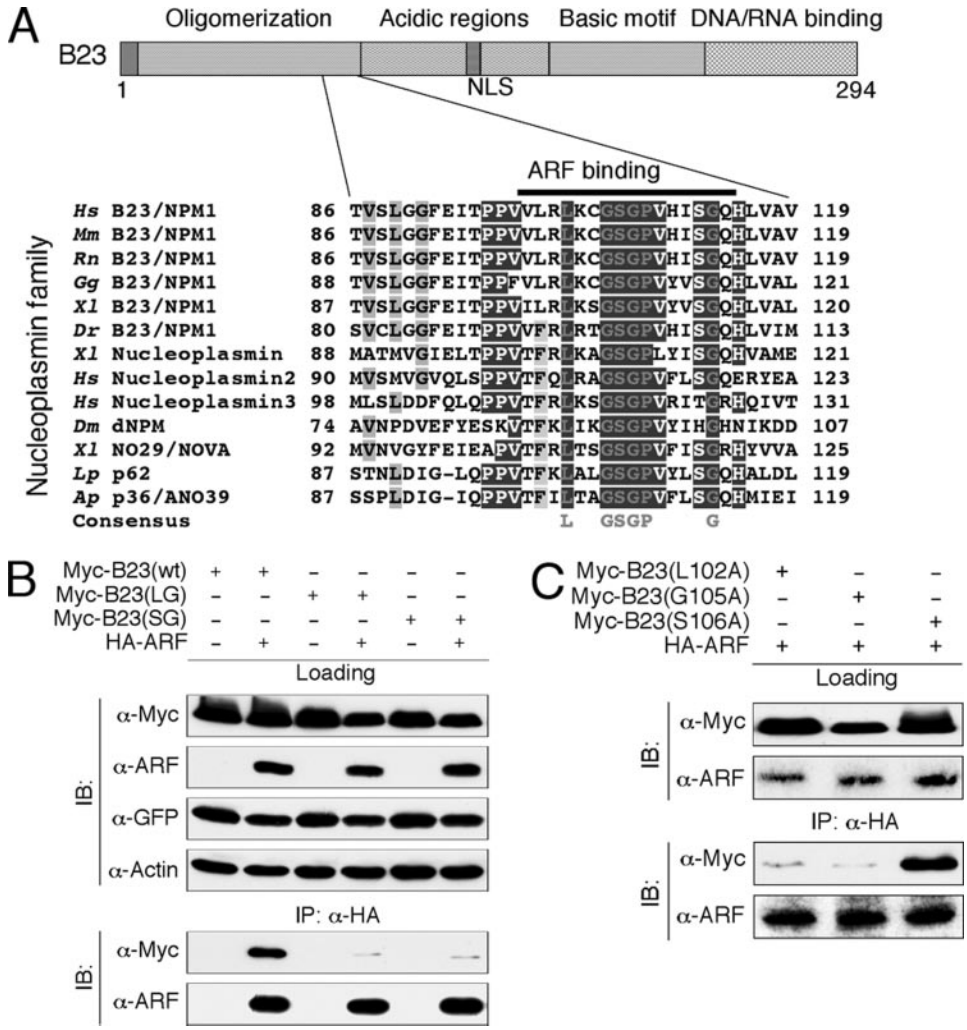

FIGURE 2. **Identification of residues in B23 required for ARF binding.** *A*, multiple sequence alignment of B23 and B23-related proteins reveals a highly conserved nucleoplasmin core in the oligomerization domain and an absolutely conserved GSGP motif (GSGP loop). *Hs*, *Homo sapiens*; *Mm*, *Mus musculus*; *Rn*, *Rattus norvegicus*; *Dr*, *Danio rerio*; *Gg*, *Gallus gallus*; *Xl*, *Xenopus laevis*; *Dm*, *Drosophila melanogaster*; *Lp*, *Lytechinus pictus* (sea urchin); *Ap*, *Asterina pectinifera* (starfish). *B* and *C*, mutations in the B23 GSGP loop disrupt ARF binding. U2OS cells were either singly transfected with plasmids encoding wild-type Myc-B23 and Myc-tagged B23 mutants or cotransfected with various B23 constructs and HA-ARF, as indicated. Immunoprecipitation and Western blotting assays were performed essentially the same as described in Fig. 1. *LG*, double substitutions of $Leu^{102} \rightarrow Ala$ and $Gly^{105} \rightarrow Ala$; *SG*, double substitutions of $Ser^{106} \rightarrow Ala$ and $Gly^{107} \rightarrow Ala$.

nuclear localization signal (NLS) sequence. The oligomerization region of B23 and nucleoplasmin is sometimes referred to as the "core." The core contains the elements necessary and sufficient for oligomerization and is presumably the critical functional unit in all members of this protein family (54). We have noticed that the minimal region in B23 (residues 100–116) required for ARF binding falls within the core domain (Fig. 2*A*). Alignment of the core from currently known members of the nucleoplasmin family identified several extremely conserved residues including a GSGP sequence (Gly^{105}–Pro^{108} in human B23) that is located in middle of the ARF binding site (Fig. 2*A*). The GSGP sequence (a.k.a. GSGP loop) has been implicated in playing a central role in the formation of nucleoplasmin oligomers (40). To determine whether the GSGP loop is involved in the ARF-B23 interaction, we constructed B23 mutants where several of the most conserved amino acid residues were replaced with alanines and tested for their interaction with ARF. Double substitutions of $Leu^{102} \rightarrow Ala$ and $Gly^{105} \rightarrow Ala$ (LG) or $Ser^{106} \rightarrow Ala$ and $Gly^{107} \rightarrow Ala$ (SG) in B23 significantly reduced ARF binding (Fig. 2*B*), indicating that the GSGP loop in B23 is critically important for mediating ARF binding. We further tested single amino acid substitutions in the GSGP loop. Single substitutions of $Leu^{102} \rightarrow Ala$ or $Gly^{105} \rightarrow Ala$ achieved a similar effect as with the double mutations in disrupting ARF binding, whereas $Ser^{106} \rightarrow Ala$ did not, even though Ser^{106} is highly conserved in the GSGP loop. A homology crystal structure model of B23 built on basis of the structure of *Xenopus* NO38 (B23 ortholog) (43) had predicted that each substitution in the GSGP loop, except for $Ser^{106} \rightarrow Ala$, would have considerable impact to the conformation of B23 (see below), which suggested that the mutations that disrupt ARF binding might have altered the core conformation of B23.

Essential Role of the ARF Binding Residues for B23 Dimerization and Oligomerization—B23 exists predominantly as an oligomer in living cells and to a lesser extent as a free monomer (55). Because the N-terminal 119 residues contain the entire B23 homo-oligomerization domain (50), we wanted to test whether any of the B23 N-terminal deletion and substitution mutants was still able to dimerize. We transiently expressed B23 N-terminal deletion mutants in U2OS cells and determined dimer formation between the mutant B23 and the endogenous B23 by immunoprecipitation Western assays. The endogenous B23 could be detected in transfections with Myc-tagged wild-type B23 and in the 1–192 fragment of B23 (indicated by arrows), but not in any of the N-terminal deletion B23 mutants (Fig. 3*A*). We noticed that deletion of the C-terminal 102 residues enhanced the dimerization between the mutant and the endogenous B23, and the reason for this remains unclear at the moment. We further tested the GSGP loop substitution mutants for their activity in dimerization. Consistent with findings from crystal structure studies of other members of the nucleoplasmin family indicating the structural importance of the GSGP loop motif (40, 42, 43), we found that the B23(LG) and B23(SG) mutants were unable to bind endogenous B23 (Fig. 3*B*). Consistent results were also obtained with bacterial produced B23 in an *in vitro* assay (Fig. 3*C*). We noted that

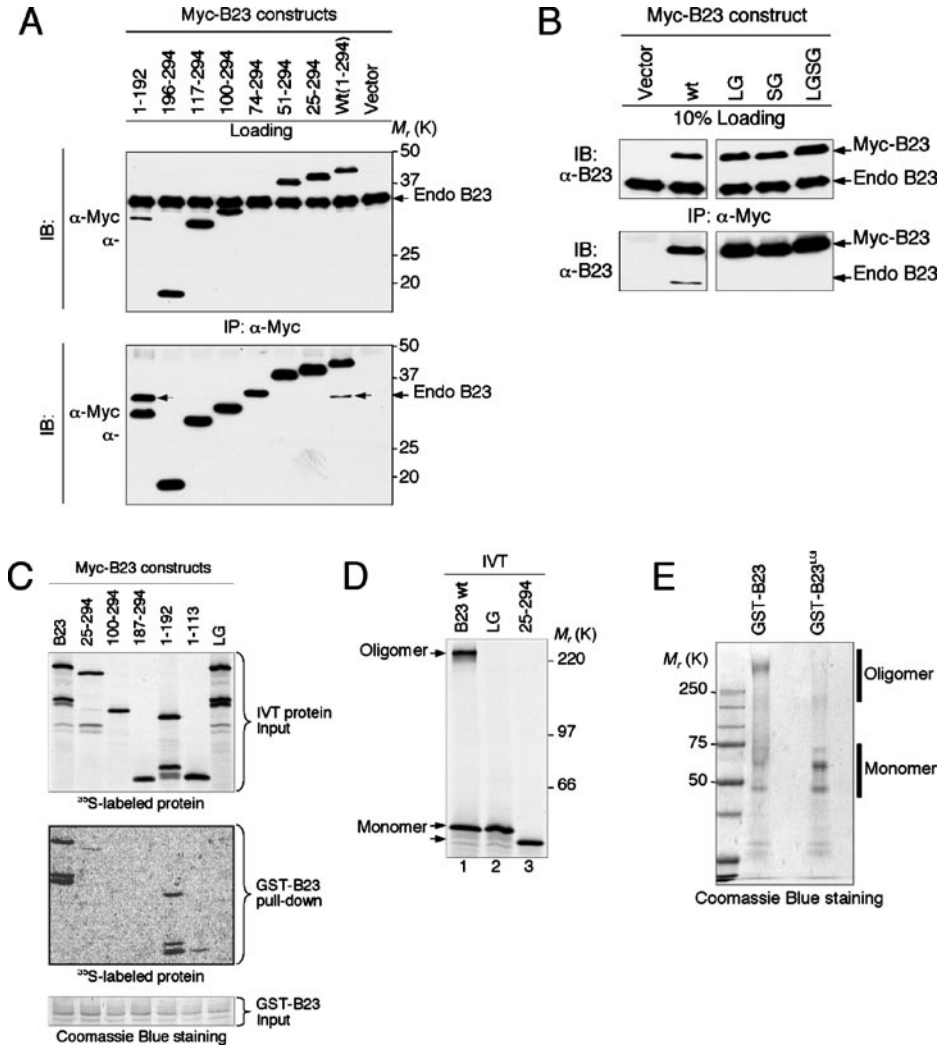

FIGURE 3. **Essential role of the ARF binding residues for B23 dimerization.** *A*, homodimer formation between ectopically expressed Myc-B23 and endogenous B23. U2OS cells were singly transfected with plasmids encoding wild-type Myc-B23 and various B23 deletion mutants. Immunoprecipitation and Western blotting were performed as described in the legend to Fig. 1, except that a mixture of anti-B23 and anti-Myc antibodies were used in the immunoblotting, as indicated. The ectopically expressed B23 was detected by anti-Myc antibody 9E10 whereas endogenous B23 was detected using an anti-B23 antibody. *Arrows* indicate endogenous B23 co-immunoprecipitated by Myc-B23. *B*, GSGP loop mutations inhibit B23 oligomerization. U2OS cells were singly transfected with plasmids encoding wild-type Myc-B23 and Myc-tagged B23 GSGP loop substitution mutants, as indicated. *C*, *in vitro* interaction of GST-B23 and ^{35}S-labeled B23 mutants. B23 protein was produced with a coupled IVT system or from bacteria as a GST-tagged protein. Equal amount of GST-B23 protein was incubated with ^{35}S-labeled wild-type B23 and various B23 mutants as indicated. GST-B23-bound radioactive B23 was detected by autoradiography. Input for ^{35}S-labeled B23 and GST-B23, are shown by autoradiography and Coomassie Blue staining respectively. Lower molecular weight bands seen in lanes with wt B23, B23-(25–294), B23-(1–192), and B23(LG) mutants represent initiation of translation *in vitro* from downstream methionine residues in B23 (in particular M1, M7), given that the Myc tag is placed at the N terminus and the first ATG (M1) in B23 cDNA is retained. *D*, homo-oligomer formation of B23 and B23 N-terminal mutants. Myc-B23 was *in vitro* translated in the presence of [^{35}S]methionine. The samples, without prior heating in SDS loading buffer so as to preserve the oligomer, were separated on an SDS-PAGE gel, and the results analyzed by autoradiography. *E*, homo-oligomer formation was analyzed essentially the same as in *D* except experiment was conducted with GST-B23 proteins.

B23-(1–113) mutant was attenuated in binding to GST-B23 (Fig. 3*C*). The reason for this remains unclear, but it could be due to the B23-(1–113) mutant lacks the last residues within the conserved B23 oligomerization domain. Notably, B23-(1–113) mutant can still bind with ARF both *in vivo* and *in vitro* (23) (data not shown). We also detected weak residual *in vitro* dimerization between B23-(25–294) and wt GST-B23. Thus, B23-(1–113) and B23-(25–294) deletion mutants behave hypomorphic, displaying different binding to itself *versus* wt B23, and also depending on the experimental system.

To determine whether the non-dimeric B23(LG) mutant also was defective in forming homo-oligomers, B23 protein was produced with either an IVT system or in bacteria as a GST-tagged fusion protein and was loaded on gels without prior boiling of the samples in SDS loading buffer. Under these conditions, the B23 oligomer was readily observed as a distinct band near the top of the gel greater than 220 kDa (Fig. 3, *D* and *E*). In contrast, the B23(LG) and the B23-(25–294) mutants were unable to form oligomers (Fig. 3, *D* and *E*). Together, these results show that the residues in B23 essential for ARF binding are also critical for B23 to form oligomers.

Modeling of B23 Core Mutants—To gain further insight into the role of the GSGP loop in mediating ARF binding, we modeled the structural basis of the B23(LG) mutant. A homology model of B23 was built on basis of the structure of NO38 core domain (43). From the high sequence homology between NO38 and human B23, we believe that the structure of B23 not only has a similar topological folding as that of NO38, but also forms a pentamer in the crystal state (Fig. 4*A*). The model shows that the GSGP loop was located on the surface of the monomer and pentamer of B23. However, the GSGP loop does not directly contribute to the interfacial interactions of the dimer or proposed decamer structure. Therefore, the impact of the mutations of L102A, G105A, and G107A on dimerization or oligomerization of B23 must be achieved via conformational changes within the monomeric B23. A careful examination of the model structure shows that Leu^{102} is a key contributor, together with Leu^{23} and Val^{109}, in forming the hydrophobic core of B23. Thus, a Leu^{102} → Ala mutation would significantly weaken the hydrophobic interactions between the GSGP loop and Leu^{23}/Val^{109} pocket and thus impact the conformation of B23 and the formation of oligomers. Gly^{105} has 104° and 149° for its backbone conformational angles of ϕ and φ, and Gly^{107} has ϕ and φ of 81° and −171°. These angles are allowed only for glycine. Thus, the Gly^{105} → A and Gly^{107} → Ala mutations would dramatically impair or even destroy the B23 monomeric β-barrel and thus the formation of oligomers. On the other hand, the structural model would predict no significant impact of the Ser^{106} → Ala mutation on the conformation of the B23 β-barrel because Ser^{106} has conformational angles of −77° and −30°, which allow for the replacement of alanine without impact on the B23 conformation. These predictions are completely consistent with the experi-

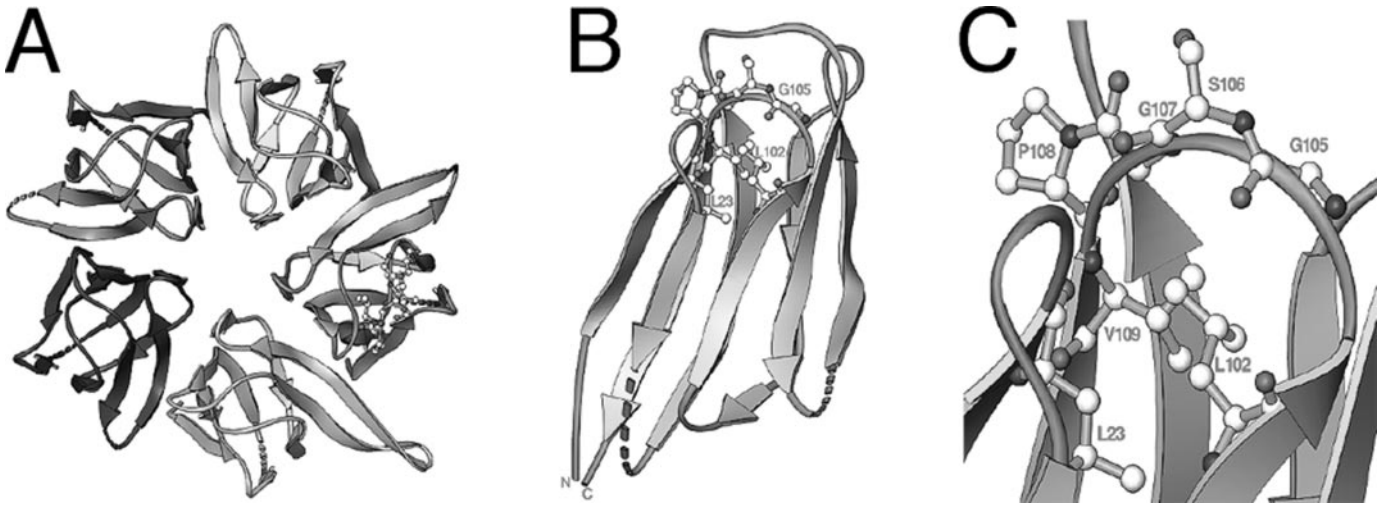

FIGURE 4. **Ribbon diagram of B23 model.** *A*, B23 pentamer. *B*, B23 monomer. The GSGP loop is shown in the *stickball model*. *C*, detailed view of the GSGP environment, where Leu[102] contributes to formation of the hydrophobic core of the B23 molecule.

mental results of Fig. 3, and suggest that the conformation of the B23 core domain is critical for mediating ARF binding.

Non-oligomeric B23 Delocalizes from the Nucleolus—Normally, B23 localizes to the nucleolus. The mechanisms governing the nucleolar localization of B23 are unknown, although it has been suggested that B23 nucleolar localization is closely associated with the states of cell growth and RNA synthesis (56). To find out whether there is a potential link between B23 oligomerization and its nucleolar localization, we determined the subcellular location of the various Myc-tagged B23 proteins in transiently transfected U2OS cells by immunofluorescence staining with an anti-Myc antibody. The B23 N-terminal deletion mutant lacking the first 24 residues, as well as the other mutants with progressive N-terminal deletions delocalized from the nucleolus and were distributed throughout the nucleus (Fig. 5*A*, *panels 1–3* and data not shown). The B23-(196–294) mutant lacking both the oligomerization domain and the nuclear localization signal (NLS) (50) dispersed throughout the nucleus and cytoplasm (Fig. 5*A*). Notably, nucleolar staining was still clearly visible in cells expressing the N-terminal deletion mutants, indicating that the proteins are not excluded from the nucleolus. This was in particular true for B23-(25–294) mutant that also showed residual binding to GST-B23 *in vitro* (Fig. 3*C*) although this interaction was not seen in the co-immunoprecipitation experiment. In contrast, the B23 C-terminal deletion mutants (1–113) and (1–192) showed nucleolar localization, but with increased nucleoplasmic staining than seen in wt B23-transfected cells (Fig. 5*A*, *panels 5* and *6*). These results are consistent with the notion that the activity of B23 oligomerization correlates with its nucleolar accumulation. In further support of this notion, B23 mutants with GSGP loop substitutions disrupting oligomerization delocalized from the nucleolus (Fig. 5*B*, *panels 2–5*), whereas the B23 mutant that did not affect oligomerization (S106A) remained in the nucleolus (Fig. 5*B*, *panel 6*). To further confirm these findings we fused wt B23 and B23(LG) mutant with GFP and analyzed the localization in living cells. In agreement with results using fixed cells, wt B23-GFP, but not the B23(LG)-GFP mutant, accumulated in nucleoli of living cells (data not shown). We noticed that the B23-(1–113) fragment lacking the NLS, yet localized to the nucleolus (Fig. 5*A*, *panel 5*). We believe this is due to its ability to oligomerize with endogenous B23. Indeed, B23-(1–113) displayed a weak binding to wt GST-B23 as in the *in vitro* binding assay (Fig. 3*C*). The results of each of the B23 mutant ability to interact with ARF, to form oligomers, and to localize to the nucleolus are summarized in Fig. 5*C*.

B23(LG) Mutant Is Defective in Restoring Cell Growth—To study the B23 and B23(LG) mutant functions in cell growth and proliferation, we used siRNA-mediated knockdown of endogenous B23 in U2OS cells followed by rescue with transient expression of GFP-tagged B23 (B23-GFP) or B23(LG) mutant (B23(LG)-GFP). Knockdown of endogenous B23 in U2OS cells impairs cell growth as measured by total cell count (Fig. 6*A*). On the other hand, ectopic expression of B23-GFP and B23(LG)-GFP slightly, but reproducibly, promoted cell growth (Fig. 6*B*). In this setting where endogenous B23 is still kept at a normal level there was no major difference between the B23(LG)-GFP mutant and B23-GFP. Interestingly, in cells depleted of endogenous B23 with siRNA the wild-type B23 was able to restore cell growth, whereas the B23(LG)-GFP mutant was not (Fig. 6*C*), indicating that the non-oligomeric B23(LG) mutant is defective in promoting cell growth.

It has been shown that B23 plays a critical role in controlling centrosome duplication and genomic stability (25, 38). To further study the functional consequences of the B23(LG) mutant, we examined nuclear integrity of cells expressing the mutant protein by scoring cells with aberrant nuclear structure. We noticed that most cells expressing B23-GFP exhibited normal nuclear appearance (Fig. 6, *D* and *E*). In contrast, a significant fraction (~15%) of cells expressing the B23(LG) mutant showed striking nuclear abnormalities, such as multiple or bi-lobed nuclei and abnormally shaped nuclei (Fig. 6, *D* and *E*). This high frequency of nuclear abnormalities was not seen in GFP- (data not shown) or B23-GFP-transfected cells.

Non-oligomeric B23 Is Unstable—B23 is a stable protein with a half-life greater than 24 h (23). One of the probable reasons for this stability could be its localization in the nucleolus, where no protein degradation has been found. With the finding that the non-oligomeric B23 delocalizes from the nucleolus, we wanted to determine whether there is a link between nucleolar localization and B23 stability. To this end, we determined the half-life of B23 with a pulse chase experiment. The B23 proteins were transiently expressed in U2OS cells, pulse-labeled with [^{35}S]methionine, and the protein half-life was chased for up to 40 h. Consistent with previous observation (23), the wild-type B23 was a stable protein, with a half-life greater than 32 h (Fig. 7*A*). The C-terminal deletion mutant B23 (1–192) was also a very stable protein with a half-life at least as long as that of the wild-type B23 (Fig. 7*A*). In contrast, B23 mutants with N-terminal deletions or GSGP loop mutations were much shorter lived relative to wt B23, with half-lives around 10 h (Fig. 7*A*). The half-lives of these non-oligomeric B23 mutants were similar to the half-

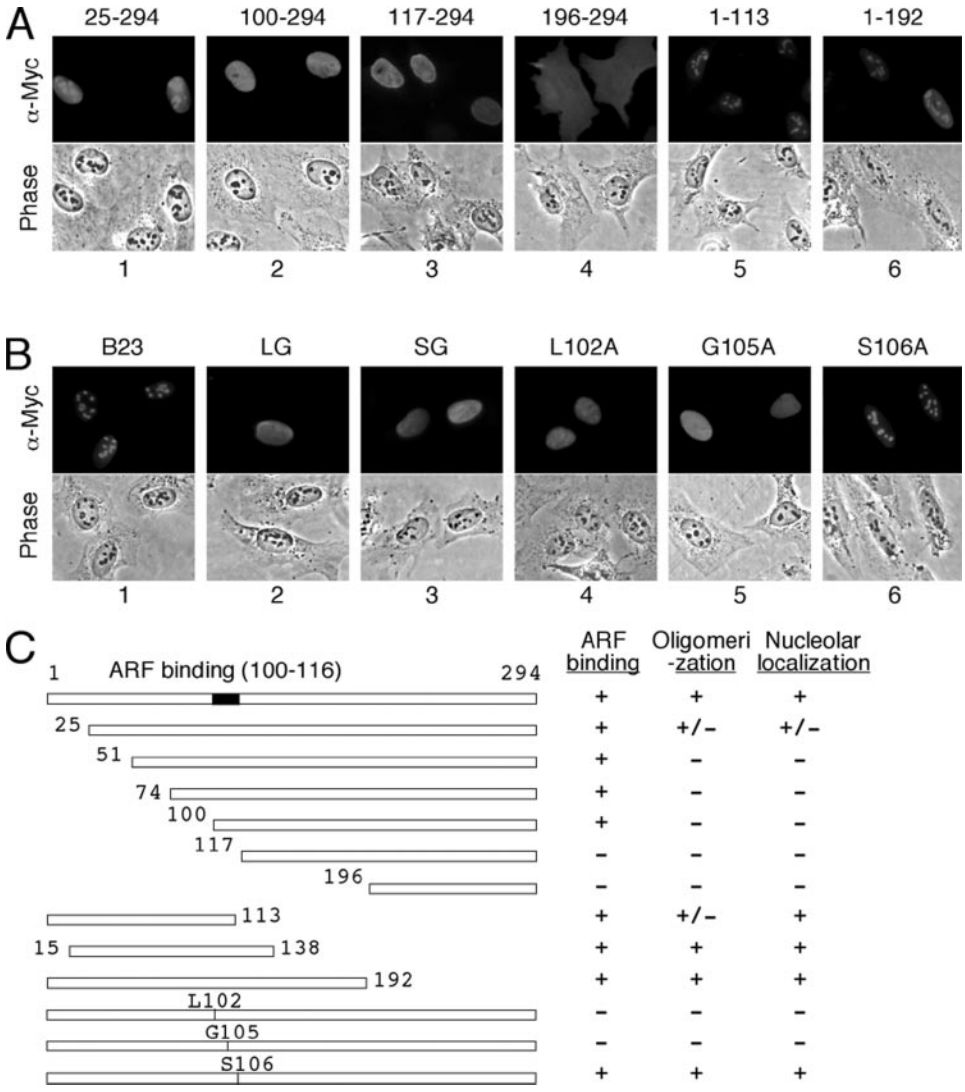

FIGURE 5. **Non-oligomeric B23 delocalizes from the nucleolus.** *A*, B23 N-terminal deletion mutants delocalize from the nucleolus. U2OS cells were singly transfected with indicated Myc-tagged B23 plasmids. 24 h after transfection, cells were fixed and immunofluorescence-stained with a rabbit anti-Myc antibody followed by staining with Texas-red-conjugated donkey anti-rabbit secondary antibody. Phase contrast images are also shown. *B*, B23 GSGP loop mutants delocalize from the nucleolus. The assay was performed essentially the same as in *A*. *C*, schematic representation of the ARF binding, oligomerization, and nucleolar localization properties of various Myc-B23 mutants. The ARF binding site on B23 (residues 100–116) is indicated.

life of a wild-type B23 with ARF overexpression, which has been determined to be about 12 h (23). Thus, B23 mutants that are unable to oligomerize delocalize from the nucleolus and are more rapidly degraded.

To determine whether nucleolar localization and oligomerization are both required for B23 to be a stable protein, we took advantage of treating cells with a low concentration of actinomycin D (5 nM), which is known to delocalize B23 from the nucleolus (57). U2OS cells were treated with 5 nM actinomycin D for 12 h to induce a delocalization of B23, followed by a B23 half-life assay. The actinomycin D treatment delocalized endogenous B23 from the nucleolus to the nucleoplasm (Fig. 7*B*), a location reminiscent of that of mutant B23 with GSGP loop mutations (Fig. 5*B*). The treatment did not affect B23 dimerization as determined by dimer formation between endogenous B23 and transfected Myc-tagged B23 (Fig. 7*C*), suggesting that B23 dimerization can occur outside of the nucleolus. In addition, under these conditions the B23(LG) mutant and the endogenous B23 co-localized to the same compartment, yet they did not interact, further confirming the lack of dimerization activity of the B23(LG) mutant. Nor did actinomycin D treatment affect the B23 steady state level as determined by a Western assay (Fig. 7*D*), or its half-life as indicated by a ^{35}S pulse-chase assay (Fig. 7*E*), demonstrating that delocalization from the nucleolus *per se* does not trigger rapid degradation of B23. Hence, the decreased half-life of the non-oligomeric B23 mutants most likely resulted from their inability to form oligomers together with a nucleoplasmic localization. However, we cannot rule out the effect of conformational changes on B23 stability, which occur hand-in-hand with a failure to oligomerize. Identification of a monomeric B23 mutant that retains a wild-type conformation could resolve this issue but remains a formidable challenge if even possible. Finally, we noticed that the half-life of the endogenous B23 was longer than that of transfected wild-type B23 (compare Fig. 7, *A* with *E*). This is presumably because of the fact that endogenous B23 could more efficiently form oligomers than the transfected B23, which may have been expressed at a non-physiological high level.

The increased instability of B23 core mutants could be due to increased ubiquitination and proteasomal degradation. To test this possibility, U2OS cells were transfected with plasmids encoding wt B23 or B23(LG) mutant. After 20 h, cells were treated for an additional 6 h with MG132 proteasome inhibitor followed by harvest directly into Laemmli sample buffer with SDS. As can be seen in Fig. 8*A*, wt B23 remained stable and changed very little in level in response to MG132 treatment. In contrast, the B23(LG) mutant was readily stabilized by MG132, suggesting that the instability of the B23 core mutants is at least in part mediated through proteasomal degradation. To further investigate the putative role of proteasome-mediated degradation of B23 core mutants, an *in vivo* ubiquitination assays was carried out. U2OS cells were co-transfected with plasmids encoding HA-tagged poly-ubiq-

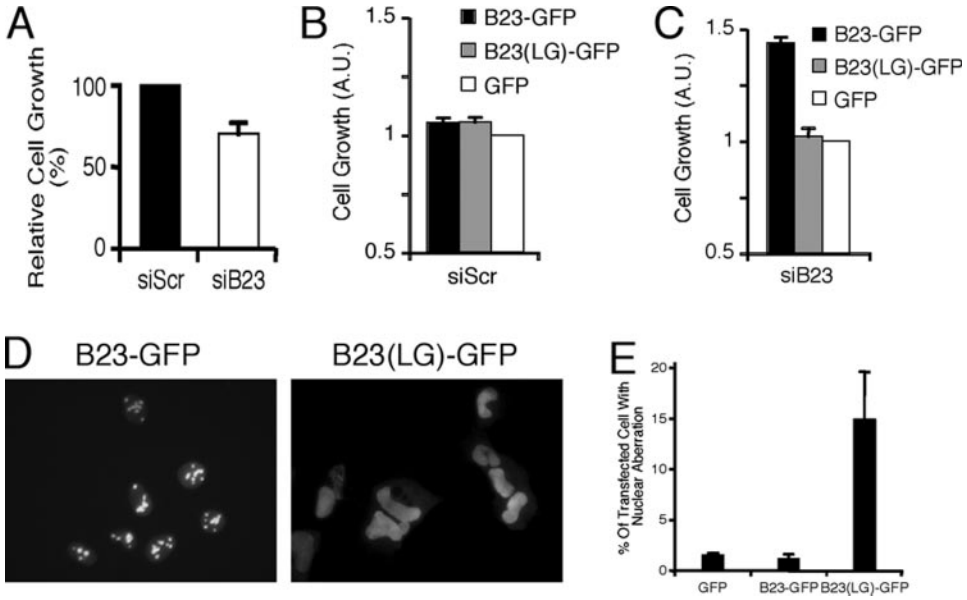

FIGURE 6. **B23 mutant is defective in restoring cell growth.** *A*, knockdown of B23 in U2OS cells with a B23 siRNA oligo impairs cell growth. Data presented as relative cell number seen in siB23 oligo-transfected cells compared with control cells transfected with scrambled siRNA (*siScr*) set to 100%, 72 h after siRNA transfection. An average of three experiments is shown. *B*, transient expression of B23-GFP, B23(LG)-GFP but not GFP alone in U2OS cells promote cell growth. U2OS cells were transfected with indicated plasmid DNA for 24 h and analyzed using absorbance 595 nm measurements (Bradford assay) of total protein. Shown is one representative experiment in triplicate, and data are presented relative to GFP-transfected cells. *A.U.*, arbitrary units. *C*, depletion of B23 in U2OS cells with a B23 siRNA or a control siRNA (*siScr*) for 72 h was followed by transfection with B23-GFP, B23(LG)-GFP, or GFP alone. Data were presented as in *B*. Transfection of GFP or control siRNA did not have discernible effect on cells (data not shown). *D*, 24 h after transfection of U2OS cells with GFP, B23-GFP or B23(LG)-GFP plasmids, cells were fixed and counterstained with DAPI. Cells expressing B23(LG)-GFP but not B23-GFP displayed nuclear abnormalities such as multiple or bi-lobed nuclei, abnormally shaped or enlarged nuclei. *E*, quantification of immunostaining data in *D*, presented as the percentage of transfected cells showing nuclear abnormalities for GFP, B23-GFP, or B23(LG)-GFP. At least 400 transfected cells were counted and analyzed for each construct. Shown is one representative experiment in triplicate.

uitin and B23 or B23 mutants followed by denaturing cell lysis and immunoprecipitation. Before harvest, all samples were treated with MG132 to allow accumulation and detection of B23 ubiquitin conjugates. Under normal conditions the level of ubiquitin conjugation to wt B23 was low or undetectable even after 10 h of treatment with MG132, in agreement with the long half-life and nucleolar localization of B23 (Fig. 8*B*). In contrast, GSGP loop mutants B23(SG) and B23(LG) displayed a markedly increased level of ubiquitination (Fig. 8*B*). We conclude that B23 GSGP loop mutants are less stable relative to wt B23 because of increased ubiquitination and proteasome-mediated degradation.

DISCUSSION

It has recently been shown by several groups that the tumor suppressor ARF interacts with the nucleolar protein B23/NPM (23, 44–46). Although these studies agreed upon mapping of the ARF N-terminal as the binding domain, they came to distinct conclusions about the region in B23 that is required for the interaction. Bertwistle *et al.* (45) suggested a direct binding to the acidic domain with a requirement for the oligomerization domain, Itahana *et al.* pinpointed the N-terminal region 1–113 (23), whereas Korgaonkar *et al.* (46), using an *in vitro* binding assay, suggested a region in B23-(187–295) known to harbor the heterodimerization and nucleic acid binding domains. We noted several potential problems in mapping the ARF binding site on B23. The first problem is the tendency of binding of the exogenous B23 to endogenous B23 through the oligomerization domain so that the endogenous B23 might bridge ARF to the exogenous B23; such an interaction might cause confusion if the results are not interpreted cautiously, as also pointed out by Korgaonkar *et al.* This is particularly a problem when taking into consideration that the endogenous B23 is a highly abundant protein in the cell, expressed at similar or higher levels than ectopically expressed B23 (see Fig. 3). Second, B23 exists in large RNP complexes; therefore proteins that do not bind directly can be linked and immunoprecipitated through RNA and other proteins in mild IP conditions. Third, localization of B23 mutants (nucleolus *versus* nucleoplasm) and fourth, the binding stoichiometry of oligomeric *versus* monomeric B23 might also affect the readout in an immunoprecipitation assay.

To initially clarify the ARF-B23 binding issue and to use ARF as a binding substrate for the continued study of B23 function, we generated a broad series of B23 deletion mutants and carried out both *in vivo* and *in vitro* binding assays in an attempt to define the ARF binding site on B23. Bertwistle *et al.* (45) suggested that ARF binds the acidic regions in B23 with an "undefined contribution" from the oligomerization domain. We found that this "undefined contribution" can be narrowed down to B23 amino acid residues 100–117. We also confirmed our previous study showing that ARF can directly bind the B23 oligomerization domain (see below) without the presence of the acidic regions. However, our data cannot rule out the possibility that the acidic patches may increase and stabilize the ARF binding. We also demonstrated that ARF is able to bind monomeric B23, by using several B23 N-terminal deletion mutants, which are devoid of dimerization/oligomerization. The C-terminal region of B23 could contain another ARF binding site, since we confirmed that a fragment of 187–294 of B23 interacted with ARF in an *in vitro* GST pull-down assay, consistent with the finding by Korgaonkar *et al.* (46). However, we observed binding of the C-terminal fragment of B23 with ARF only when B23 was produced as a GST fusion protein and mixed with *in vitro* translated ARF. *In vitro* translated B23-(187–294) fragment did not interact with GST-ARF whereas the N-terminal region of B23-(1–113) was able to do so (data not shown). It is possible that the recombinant B23 mutant produced *in vitro* might not be properly modified and/or folded, creating an aberrant interaction with ARF. Supporting this view, interaction with ARF is not really evident with the GST-B23-(120–294) fragment (Fig. 1*D*).

Having established the importance of the B23 region 100–117 in ARF binding, we made a comparative sequence alignment analysis of multiple members of the nucleoplasmin family. Intriguingly, this region turned out to be the most conserved region in the whole nucleoplasmin

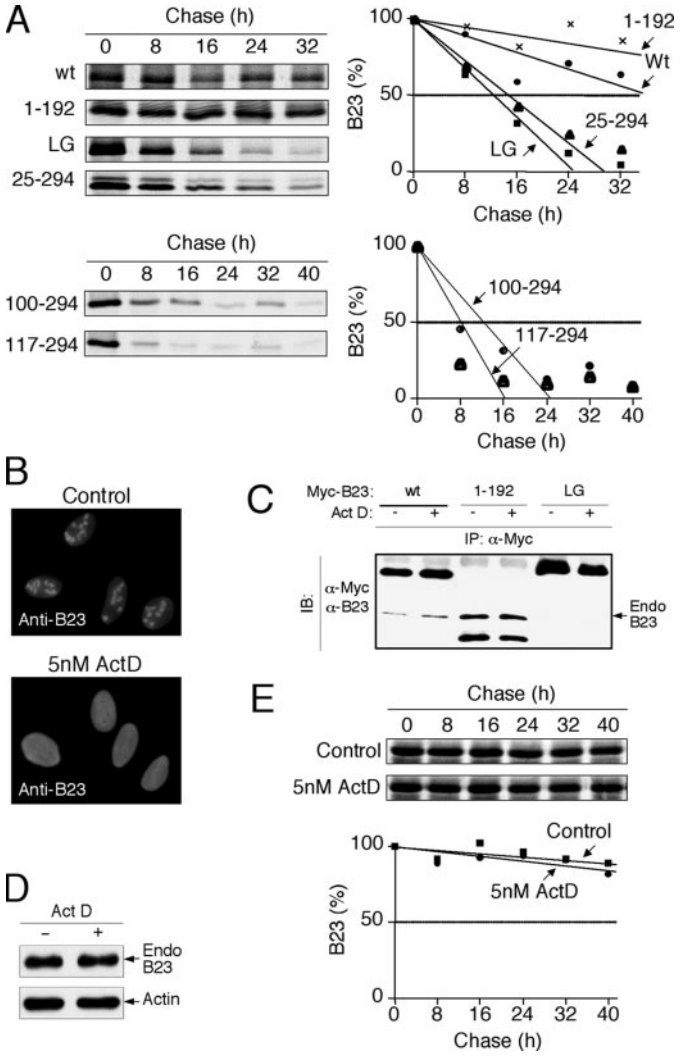

FIGURE 7. **Non-oligomeric B23 is unstable.** *A*, half-life determination of various B23 proteins. U2OS cells were singly transfected with plasmids encoding Myc-tagged wild-type B23 (wt), the C-terminal deletion mutant B23-(1–192), the GSGP loop substitution mutant B23(LG), and N-terminal deletion mutants B23-(25–294), B23-(100–294), and B23-(117–294). Twenty hours after transfection, cells were pulse-labeled with [^{35}S]methionine for 2 h and then chased for the indicated length of time. Cell lysates were immunoprecipitated with an anti-Myc antibody. The resulting B23 immunoprecipitates were separated by SDS-PAGE and visualized by autoradiography. The amount of labeled B23 protein at each time point was quantified on a PhosphorImager and normalized relative to the amount of radiolabeled B23 present in cells following the 0 h chase; results are plotted. *B*, localization of endogenous B23 in U2OS cells after treatment with 5 nM actinomycin D for 12 h. Immunofluorescence staining was performed essentially the same as described in Fig. 5. *C*, U2OS cells were singly transfected with plasmids encoding the Myc-tagged wt B23, C-terminal deletion mutant B23-(1–192), or GSGP loop mutant B23(LG). Twenty-four hours after transfection, cells were either untreated (−) or treated (+) with 5 nM actinomycin D. Immunoprecipitation and Western blotting assays were performed essentially the same as described in the legends to Figs. 1 and 2. *D*, level of endogenous B23 was not affected by 5 nM actinomycin D treatment for 12 h. *E*, B23 half-life assay after 5 nM actinomycin D treatment. U2OS cells were treated with 5 nM actinomycin D for 6 h; cells were then pulse-labeled with [^{35}S]methionine for 2 h and chased for the indicated length of time. Cell lysates were assayed as described above.

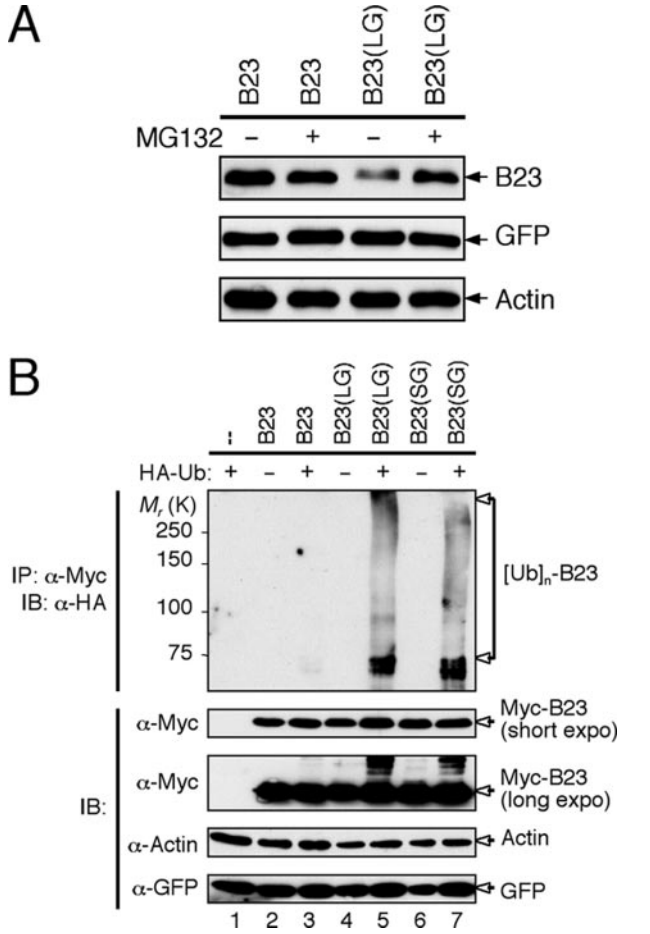

FIGURE 8. **Ubiquitination of B23 GSGP-loop mutants.** *A*, MG132 treatment stabilizes B23(LG) mutant but not wild-type B23. U2OS cells were transfected with plasmids encoding wt B23 or B23(LG) mutant together with GFP as a transfection marker. After 20 h, the transfected cells were treated with or without MG132 for an additional 6 h. Following whole cell extract preparation in SDS buffer the lysates were analyzed by Western blot using antibodies against Myc, GFP, or actin. One out of three experiments, with similar results is shown. *B*, *in vivo* ubiquitination of B23 GSGP loop mutants. U2OS cells were transfected with plasmids encoding wt B23, B23(LG), or B23(SG) mutants in combination with a plasmid for HA-tagged polyUb as indicated. Myc-tagged B23 from denatured cell lysates was immunoprecipitated with a rabbit polyclonal antibody against Myc followed by immunoblot against ubiquitin (anti-HA), Myc-B23, actin or GFP. In this experiment all samples were treated with 10 μM MG132 for 10 h before harvest.

superfamily, although some other parts of the core are also well conserved. Initial experiments were aimed at mutating single amino acid residues in this region followed by analysis of binding with ARF. We, however, also noted a number of intriguing features with these mutants. Not only did some of them lose the ability to bind ARF *in vivo*, but they also showed a striking delocalization from the nucleolus to the nucleoplasm, were less stable than the wild-type protein, and failed to dimerize both *in vivo* and *in vitro*. Based on our data, a reasonable model concerning ARF-induced B23 degradation can be proposed: ARF, through interacting with the GSGP loop in B23, might interfere with B23 dimerization/oligomerization, perhaps by inducing conformational changes or through steric hindrance. The non-oligomeric B23 may then delocalize to the nucleoplasm and undergo proteolytic degradation. That the GSGP loop mutant B23(LG) was defective in forming functional oligomers similar to wt B23 was confirmed by using GST pull-down assays, *in vitro* translation product analysis followed by non-reducing SDS-PAGE and co-immunoprecipitation assays. In support, we also modeled the structural basis of the B23 mutants, based on the structure of the *Xenopus* B23 homolog NO38 core domain (43). Predictions obtained from the structure modeling were consistent with the experimental results. In addition the modeling also suggested that it is the conformation of the B23 core domain, but may be not individual amino acid residues within, that is critical for mediating ARF binding. Given the strong similarity between the primary sequences and secondary structures of the GSGP loop among the nucleoplasmin family members, it would be of interest to find out whether ARF interacts with other members of the family. Indeed, we have found that ARF also interacts with NPM3 in a B23-free system (data not shown) and importantly, NPM3

lacks the C-terminal region that is unique to B23 (53), further indicating that ARF can interact with B23 in the absence of its C terminus. It is conceivable that mutations in the GSGP loop motif also would render other members of the NPM family functionally handicapped.

The mechanisms that control nucleolar localization of B23 appear to differ from other nucleolar proteins. Our findings confirm the notion that the nucleolar localization of B23 requires multiple functional elements besides the NLS and the basic cluster motif in the C terminus, since we found that there is also an intimate link between nucleolar accumulation and a functional oligomerization domain. Our analysis of B23 N-terminal and GSGP loop motif mutants shows that those mutants that are unable to form oligomers also are impaired in nucleolar accumulation, although not strictly excluded from nucleoli. However it can be argued, that it is not possible to distinguish between the possibility that non-oligomeric B23 mutants also have a defective conformation that in turn prevents binding to nucleolar target proteins or that oligomerization *per se* is required for B23 nucleolar accumulation. Interestingly, our work suggests an alternative explanation to the nucleoplasmic localization of B23(L102A) mutant as noted and described elsewhere (58, 59). We here suggest that the nucleolar delocalization of B23(L102A) mutant is caused by defective oligomerization and/or conformational changes in B23. Although our data do not rule out that Leu^{102} acts within a putative B23 nuclear export sequence *LXXPXXLXL* within residues 94–102, the fact that B23(L102A) localization were mimicked by our mutants B23(G105A) and B23(G107A) is intriguing.

We found that both oligomeric wild-type B23 and B23(LG) mutant both stimulated an increase in S-phase fraction and behaved similar in a long-term cell growth assay. These results suggest that B23(LG) mutant retains some of its functions and is not a "dead" mutant. Instead, the B23(LG) mutant is primarily defective for binding ARF and possibly other basic proteins *in vivo*, whereas also having a localization defect. Our data are in agreement with the established multifunctional nature of B23. For instance, the C-terminal region of B23 can bind DNA or RNA (60), whereas on the other hand, the chaperone function has been linked to the N-terminal region (50). Taken together, our data show that the highly conserved GSGP loop in the core domain of B23 is essential for mediating both ARF binding and have an essential role in controlling aspects of B23 protein structure, stability, and localization.

Acknowledgments—We thank Koji Itahana for his contribution to the study and helpful discussions and Hilary Clegg for critical reading of the manuscript.

REFERENCES

1. Ruas, M., and Peters, G. (1998) *Biochimica. et Biophysica. Acta* **1378,** F115–F177
2. Duro, D., Bernard, O., Della Valle, V., Berger, R., and Larsen, C.-J. (1995) *Oncogene* **11,** 21–29
3. Mao, L., Merlo, A., Bedi, G., Shapiro, G. I., Edwards, C. D., Rollin, B. J., and Sidransky, D. (1995) *Cancer Res.* **55,** 2995–2997
4. Stone, S., Jiang, P., Dayananth, P., Tavtigian, S. V., Katcher, H., Parry, D., Peters, G., and Kamb, A. (1995) *Cancer Res.* **55,** 2988–2994
5. Quelle, D. E., Zindy, F., Ashmun, R., and Sherr, C. J. (1995) *Cell* **83,** 993–1000
6. Weinberg, R. A. (1995) *Cell* **81,** 323–330
7. Sherr, C. J. (1996) *Science* **274,** 1672–1677
8. Levine, A. J. (1997) *Cell* **88,** 323–331
9. Adams, P. D., and Kaelin, W. G., Jr. (1998) *Curr. Opin. Cell Biol.* **10,** 791–797
10. de Stanchina, E., McCurrach, M. E., Zindy, F., Shieh, S.-Y., Ferbeyre, G., Samuelson, A. V., Prives, C., Roussel, M. F., Sherr, C. J., and Lowe, S. W. (1998) *Genes Dev.* **12,** 2434–2442
11. Zindy, F., Eischen, C. M., Randle, D. H., Kamijo, T., Cleveland, J. L., Sherr, C. J., and Roussel, M. F. (1998) *Genes Dev.* **12,** 2424–2433
12. Bates, S., Phillips, A. C., Clark, P., Stott, F., Peters, G., Ludwig, R., and Vousden, K. H. (1998) *Nature* **395,** 124–125
13. Palmero, I., Pantoja, C., and Serrano, M. (1998) *Nature* **395,** 125–126
14. Radfar, A., Unnikrishnan, I., Lee, H.-W., DePinho, R., and Rosenberg, N. (1998) *Proc. Natl. Acad. Sci. U. S. A.* **95,** 13194–13199
15. Sherr, C. J. (1998) *Genes Dev.* **12,** 2984–2991
16. Zhang, Y., Xiong, Y., and Yarbrough, W. G. (1998) *Cell* **92,** 725–734
17. Pomerantz, J., Schreiber-Agus, N., Liegeois, N. J., Silverman, A., Alland, L., Chin, L., Potes, J., Chen, K., Orlow, I., and DePinho, R. A. (1998) *Cell* **92,** 713–723
18. Honda, R., and Yasuda, H. (1999) *EMBO J.* **18,** 22–27
19. Zhang, Y., and Xiong, Y. (1999) *Mol. Cell* **3,** 579–591
20. Tao, W., and Levine, A. J. (1999) *Proc. Natl. Acad. Sci. U. S. A.* **96,** 6937–6941
21. Weber, J. D., Jeffers, J. R., Rehg, J. E., Randle, D. H., Lozano, G., Roussel, M. F., Sherr, C. J., and Zambetti, G. P. (2000) *Genes Dev.* **14,** 2358–2365
22. Sugimoto, M., Kuo, M. L., Roussel, M. F., and Sherr, C. J. (2003) *Mol. Cell* **11,** 415–424
23. Itahana, K., Bhat, K. P., Jin, A., Itahana, Y., Hawke, D., Kobayashi, R., and Zhang, Y. (2003) *Mol. Cell* **12,** 1151–1164
24. Olson, M. O., Wallace, M. O., Herrera, A. H., Marshall-Carlson, L., and Hunt, R. C. (1986) *Biochemistry* **25,** 484–491
25. Okuda, M., Horn, H. F., Tarapore, P., Tokuyama, Y., Smulian, A. G., Chan, P. K., Knudsen, E. S., Hofmann, I. A., Snyder, J. D., Bove, K. E., and Fukasawa, K. (2000) *Cell* **103,** 127–140
26. Szebeni, A., and Olson, M. O. (1999) *Protein Sci.* **8,** 905–912
27. Colombo, E., Marine, J. C., Danovi, D., Falini, B., and Pelicci, P. G. (2002) *Nat. Cell Biol.* **4,** 529–533
28. Savkur, R. S., and Olson, M. O. (1998) *Nucleic Acids Res.* **26,** 4508–4515
29. Herrera, J. E., Savkur, R., and Olson, M. O. (1995) *Nucleic Acids Res.* **23,** 3974–3979
30. Hadjiolova, K. V., Normann, A., Cavaille, J., Soupene, E., Mazan, S., Hadjiolov, A. A., and Bachellerie, J. P. (1994) *Mol. Cell. Biol.* **14,** 4044–4056
31. Feuerstein, N., and Mond, J. J. (1987) *J. Biol. Chem.* **262,** 11389–11397
32. Feuerstein, N., Spiegel, S., and Mond, J. J. (1988) *J. Cell Biol.* **107,** 1629–1642
33. Nozawa, Y., Van Belzen, N., Van der Made, A. C., Dinjens, W. N., and Bosman, F. T. (1996) *J. Pathol.* **178,** 48–52
34. Kondo, T., Minamino, N., Nagamura-Inoue, T., Matsumoto, M., Taniguchi, T., and Tanaka, N. (1997) *Oncogene* **15,** 1275–1281
35. Higuchi, Y., Kita, K., Nakanishi, H., Wang, X. L., Sugaya, S., Tanzawa, H., Yamamori, H., Sugita, K., Yamaura, A., and Suzuki, N. (1998) *Biochem. Biophys. Res. Commun.* **248,** 597–602
36. Wu, M. H., Chang, J. H., and Yung, B. Y. (2002) *Carcinogenesis* **23,** 93–100
37. Colombo, E., Bonetti, P., Lazzerini Denchi, E., Martinelli, P., Zamponi, R., Marine, J. C., Helin, K., Falini, B., and Pelicci, P. G. (2005) *Mol. Cell. Biol.* **25,** 8874–8886
38. Grisendi, S., Bernardi, R., Rossi, M., Cheng, K., Khandker, L., Manova, K., and Pandolfi, P. P. (2005) *Nature* **437,** 147–153
39. Dingwall, C., and Laskey, R. A. (1990) *Semin. Cell Biol.* **1,** 11–17
40. Dutta, S., Akey, I. V., Dingwall, C., Hartman, K. L., Laue, T., Nolte, R. T., Head, J. F., and Akey, C. W. (2001) *Mol. Cell* **8,** 841–853
41. Shackleford, G. M., Ganguly, A., and MacArthur, C. A. (2001) *BMC Genomics* **2,** 8
42. Namboodiri, V. M., Dutta, S., Akey, I. V., Head, J. F., and Akey, C. W. (2003) *Structure (Camb.)* **11,** 175–186
43. Namboodiri, V. M., Akey, I. V., Schmidt-Zachmann, M. S., Head, J. F., and Akey, C. W. (2004) *Structure (Camb.)* **12,** 2149–2160
44. Brady, S. N., Yu, Y., Maggi, L. B., Jr., and Weber, J. D. (2004) *Mol. Cell. Biol.* **24,** 9327–9338
45. Bertwistle, D., Sugimoto, M., and Sherr, C. J. (2004) *Mol. Cell. Biol.* **24,** 985–996
46. Korgaonkar, C., Hagen, J., Tompkins, V., Frazier, A. A., Allamargot, C., Quelle, F. W., and Quelle, D. E. (2005) *Mol. Cell. Biol.* **25,** 1258–1271
47. Bhat, K. P., Itahana, K., Jin, A., and Zhang, Y. (2004) *EMBO J.* **23,** 2402–2412
48. Jones, T. A., Zou, J. Y., Cowan, S. W., and Kjeldgaard. (1991) *Acta Crystallogr. A.* **47,** 110–119
49. Carson, M. (1996) *J. Comput. Aided Mol. Des.* **10,** 273–283
50. Hingorani, K., Szebeni, A., and Olson, M. O. (2000) *J. Biol. Chem.* **275,** 24451–24457
51. Chan, W. Y., Liu, Q. R., Borjigin, J., Busch, H., Rennert, O. M., Tease, L. A., and Chan, P. K. (1989) *Biochemistry* **28,** 1033–1039
52. Burns, K. H., Viveiros, M. M., Ren, Y., Wang, P., DeMayo, F. J., Frail, D. E., Eppig, J. J., and Matzuk, M. M. (2003) *Science* **300,** 633–636
53. Huang, N., Negi, S., Szebeni, A., and Olson, M. O. (2005) *J. Biol. Chem.* **280,** 5496–5502
54. Dingwall, C., Sharnick, S. V., and Laskey, R. A. (1982) *Cell* **30,** 449–458
55. Chan, P. K., and Chan, F. Y. (1995) *Biochim. Biophys. Acta* **1262,** 37–42
56. Yung, B. Y., Bor, A. M., and Chan, P. K. (1990) *Cancer Res.* **50,** 5987–5991
57. Chan, P. K., Bloom, D. A., and Hoang, T. T. (1999) *Biochem. Biophys. Res. Commun.* **264,** 305–309
58. Wang, W., Budhu, A., Forgues, M., and Wang, X. W. (2005) *Nat. Cell Biol.* **7,** 823–830
59. Falini, B., Bolli, N., Shan, J., Martelli, M. P., Liso, A., Pucciarini, A., Bigerna, B., Pasqualucci, L., Mannucci, R., Rosati, R., Gorello, P., Diverio, D., Roti, G., Tiacci, E., Cazzaniga, G., Biondi, A., Schnittger, S., Haferlach, T., Hiddemann, W., Martelli, M. F., Gu, W., Mecucci, C., and Nicoletti, I. (2006) *Blood* **107,** 4514–4523
60. Dumbar, T. S., Gentry, G. A., and Olson, M. O. (1989) *Biochemistry* **28,** 9495–9501